

# Controllable Pt Nanoparticle Deposition on Carbon Nanotubes as an Anode Catalyst for Direct Methanol Fuel Cells

Yongyan Mu,<sup>†</sup> Hanpu Liang,<sup>†</sup> Jinsong Hu,<sup>†</sup> Li Jiang,<sup>‡</sup> and Lijun Wan\*

*Institute of Chemistry, Chinese Academy of Sciences (CAS), Beijing 100080, China*

*Received: September 29, 2005*

We report a novel process to prepare well-dispersed Pt nanoparticles on CNTs. Pt nanoparticles, which were modified by the organic molecule triphenylphosphine, were deposited on multiwalled carbon nanotubes by the organic molecule, which acts as a cross linker. By manipulating the relative ratio of Pt nanoparticles and multiwalled carbon nanotubes in solution, Pt/CNT composites with different Pt content were achieved. The so-prepared Pt/CNT composite materials show higher electrocatalytic activity and better tolerance to poisoning species in methanol oxidation than the commercial E-TEK catalyst, which can be ascribed to the high dispersion of Pt nanoparticles on the multiwalled carbon nanotube surface.

## Introduction

To satisfy mankind's ever-increasing energy needs and tackle the daunting environmental issues, one has to consider alternative energy sources to replace the currently dominant fuels, petroleum and natural gas. Direct methanol fuel cells (DMFCs), which provide a new way to store and convey energy, have attracted much attention as green power sources for automobiles and portable electronics.<sup>1–3</sup> In this electrochemical cell, methanol is directly oxidized with air to carbon dioxide and water to produce electricity. DMFC can use alkaline electrolyte. However, the carbonation of carbon dioxide is a serious problem of DMFCs in an alkaline electrolyte, which decreases the fuel cell efficiency by decreasing the electrolyte conductivity and increasing the concentration polarization.<sup>2,4</sup> Therefore, the practical DMFCs now operate with acid electrolyte, which are carbon dioxide rejecting. One of the challenges in developing DMFCs with acid media is to enhance the exchange current density due to the low reactivity of methanol oxidation in acid electrolyte.<sup>4</sup> To date, the most promising catalytic materials used for the methanol oxidation at room temperature are supported Pt catalyst.<sup>5–11</sup> It is well-known that the specific activity of catalysts is strongly related to their size, distribution, and the support. Highly distributed catalyst nanoparticles with small size and narrow size distribution are ideal for high electrocatalyst activity owing to their large surface-to-volume ratio. Among the possible supports, carbon black has been widely used as an electrode, which disperses Pt nanoparticles,<sup>4–5,12,13</sup> but carbon nanotubes (CNTs) are considered to be a more attractive candidate owing to their outstanding mechanical characteristics such as high tensile strength coupled with high surface area, high electric conductivity, and thermal conductivity.<sup>14–16</sup> Pt nanoparticles on the external walls are easier to make contact with the reactant than those trapped in the pores of the carbon black electrode. However, the effective attachment of Pt nanoparticles uniformly dispersed onto CNTs remains a formidable challenge because of the inertness of the CNT walls.<sup>17–21</sup> So far, the most established protocol for catalytic metal

immobilization on CNTs includes generating functional groups on the external walls, mostly by harsh oxidative treatments such as refluxing in HNO<sub>3</sub>, and then deposition of metals on activated CNT walls.<sup>18–23</sup> Such surface functionalization provides an avenue for metal precursors to correlate with CNTs and prompts the deposition of metal on the external walls. While these strategies are effective, the controllability has not been fully realized. The other approaches, such as physical evaporation,<sup>24,25</sup> electroless deposition,<sup>26,27</sup> and electrodeposition,<sup>28,29</sup> were also reported recently. Close examination of the existing methods reveals that they involved either a tedious pretreatment procedure to modify CNT walls or complex equipment to achieve high dispersion of Pt nanoparticles on CNTs. Therefore, it is desirable to develop a simple and effective synthetic route that provides well-dispersed Pt nanoparticles while maintaining some degree of control of particle size and size distribution on CNTs.

In this paper, we report a novel process to prepare well-dispersed Pt nanoparticles on multiwalled CNTs (MWCNTs). Different from the methods reported, which produce Pt/CNT composite by modifying CNTs to achieve high Pt dispersion, the method we adopted was to modify Pt nanoparticles with organic molecule triphenylphosphine (PPh<sub>3</sub>). In contrast to CNTs, the functionalization of Pt nanoparticles was facile and effective under much more benign conditions, such as no harsh acid and room temperature. Pt nanoparticles prepared in ethylene glycol kept their small particle size and narrow size distribution after being modified with PPh<sub>3</sub> and deposited on the surface of CNTs. Transmission electron microscopy (TEM) and high-resolution transmission electron microscopy (HRTEM) characterization were carried out to determine the particle size and distribution of the Pt catalyst. The so-prepared Pt/CNT composite materials showed higher electrocatalytic activity in methanol oxidation than the commercial catalyst.

## Experimental Section

**Nanoparticle Synthesis.** Pt nanoparticles were synthesized according to Wang's method,<sup>30</sup> details of which are as follows. An ethylene glycol solution of H<sub>2</sub>PtCl<sub>6</sub>·6H<sub>2</sub>O (50 mL, 1.93 mM) was mixed with an ethylene glycol solution of NaOH (50 mL, 0.5 M) with magnetic stirring. This makes a transparent yellow solution. Then the solution was refluxed at 160 °C for 3 h with

\* To whom correspondence should be addressed. E-mail: wanlijun@iccas.ac.cn.

<sup>†</sup> Also at the Graduate School of CAS, Beijing 100064, China

<sup>‡</sup> Current address: Schlumberger-Doll research, Ridgefield, CT 06877.

the protection of  $N_2$ . The color of the solution began to change at around 130 °C, implying that Pt precursors were being reduced and Pt nanoparticles were synthesized. The obtained Pt colloidal solution is dark brown and homogeneous.

**Modification of Pt Nanoparticles.** The obtained Pt colloidal solution (10 mL) was added to 40 mL of ethanol. Then the mixed solution was added into a toluene solution of  $PPh_3$  (50 mL, 3.81 mM) with stirring. A homogeneous, dark brown solution was obtained. After 15 min, 50 mL of distilled water was added to the solution. A liquid in two phases was obtained. The upper dark-brown solution was  $PPh_3$ -modified Pt/toluene solution and the bottom colorless solution was the mixed solution of water and ethanol. The  $PPh_3$ -modified Pt/toluene solution was washed with distilled water three times to remove the ethylene glycol and transfer the Pt nanoparticles from glycol solution to toluene, which is essential for the deposition of Pt nanoparticles on CNT walls.

**Deposition of Pt Nanoparticles on CNTs.** MWCNTs were used ultrasonically as received in toluene solution for 4 h to break big CNT aggregates and disperse CNTs. Then  $PPh_3$ -modified Pt/toluene solution was added to the CNT/toluene solution and the mixture was ultrasonicated for 5 days until all Pt nanoparticles were deposited on CNTs. The toluene solution became colorless, suggesting that the  $PPh_3$ -modified Pt nanoparticles were completely deposited on the surface of CNTs. The Pt/CNT composite was separated from the solution by centrifugation and washed by toluene three times.

**Characterization.** The size of the Pt nanoparticles and morphology of the Pt/CNT composite were observed by TEM and HRTEM. TEMs were performed on a JEOL2010 equipped with an energy-dispersive X-ray analyzer (Phoenix) (200 KV). HRTEM was carried out on a Philips F30 with an acceleration voltage of 300 kV. For TEM observation, the samples were dispersed in ethanol by ultrasonic treatment and dropped on copper grids with carbon films followed by solvent evaporation in air at room temperature. X-ray powder diffractions (XRD) were carried out on a Rigaku D/max-2500, using filtered  $Cu K\alpha$  radiation.

Electroactivities of the catalyst were measured by cyclic voltammetry with use of a three-electrode test cell at room temperature after the Pt/CNT composite was calcined at 400 °C for 1 h to remove  $PPh_3$ . A thin film electrode technique was used to make the measurements. A glassy carbon disk (3 mm in diameter) held in a Teflon cylinder was used as the working electrode, on which a thin layer of Nafion-impregnated catalyst was cast. The Pt loading of both catalysts on electrode was 1  $mg/cm^2$ . A Pt wire served as the counter electrode and a saturated calomel electrode (SCE) was used as the reference electrode. The electrolyte for electrochemical measurements was a solution of 2 M methanol in 1 M  $H_2SO_4$ . The solution was deaerated with ultrahigh-purity  $N_2$  before scanning.

## Results and Discussion

In view of the inertness of CNT walls, we prepared Pt colloidal solution in toluene, which is an excellent solvent to wet CNTs. As illustrated in Figure 1, the organic molecule  $PPh_3$  acts as a cross linker for Pt nanoparticles and CNTs. At the end of the molecule, the free electron pair of P interacts with the space orbital of Pt to form a coordination compound. And at the other end of the molecule, the phenyl rings correlate with the backbone of CNTs. There are three functions of  $PPh_3$ . At first, it causes Pt nanoparticles transfer from glycol solution to toluene solution. Second, it prevents Pt nanoparticles from aggregating with each other either in toluene solution or on the

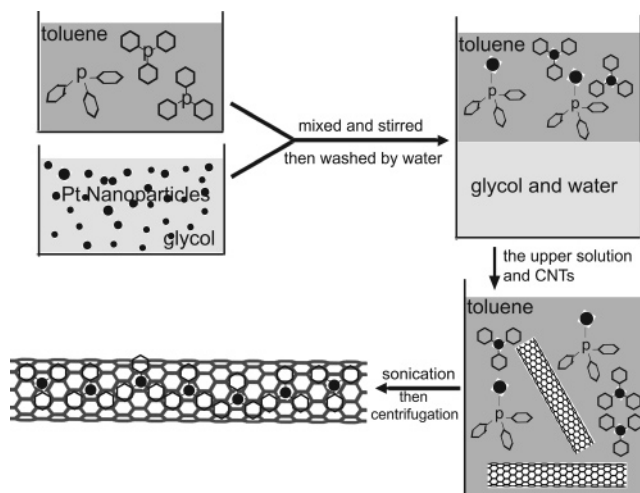


**Figure 1.** Schematic illustrations of the synthesis procedures of Pt/CNT composite.

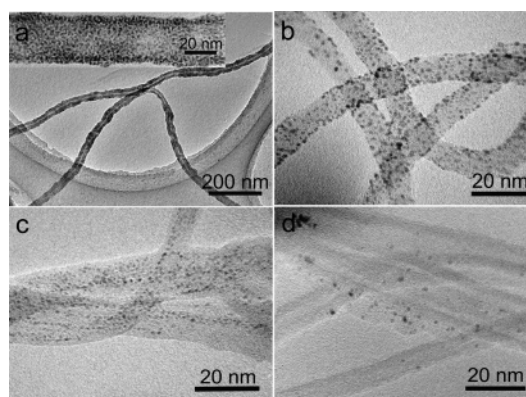


**Figure 2.** TEM images of Pt/CNT composite with different Pt content: 40.6 (a) (inset: enlarged image of panel a), 24.0 (b), 19.1 (c), and 3.1 wt % (d).

CNTs surface. At last, it links Pt nanoparticles with CNTs and leads to the uniform dispersion of Pt nanoparticles on CNT surfaces.

Pt/CNT composites with different Pt content having distinct application potential were produced by simply manipulating the ratio of Pt nanoparticles vs CNTs in solution. The as-prepared Pt/CNT composite nanomaterials were investigated by TEM. Figure 2a–d shows representative TEM images of as-prepared Pt/CNT composite with varying content of Pt, from (a) 40.6, (b) 24.0, (c) 19.1, to (d) 3.1 wt %, respectively. Figure 2a is a typical TEM image showing the CNTs covered with a continuous Pt nanoparticle adlayer, which extends the overall length of CNTs. Owing to no pretreatment, the CNTs are flexible and as long as several tens of micrometers. The insert in Figure 2a is a high-magnification TEM image of the Pt/CNT composite nanomaterials. It can be seen that there exists a well-dispersed Pt nanoparticle adlayer on the wall of a CNT. The  $PPh_3$  molecules effectively isolated adjacent Pt nanoparticles. Therefore, Pt nanoparticles are distributed on tube walls quite uniformly and do not aggregate with each other to form larger clusters. The average distance between Pt nanoparticles is less than 1 nm, which is consistent with the stabilizer  $PPh_3$  molecules.

As the content decreases, Pt nanoparticles randomly deposit on the wall of CNTs and no continuous layer can be found on the CNT surface as shown in Figure 2, panels b to d. However, no free Pt nanoparticles can be resolved in these four TEM images. It is evident that Pt nanoparticles strongly adsorb on

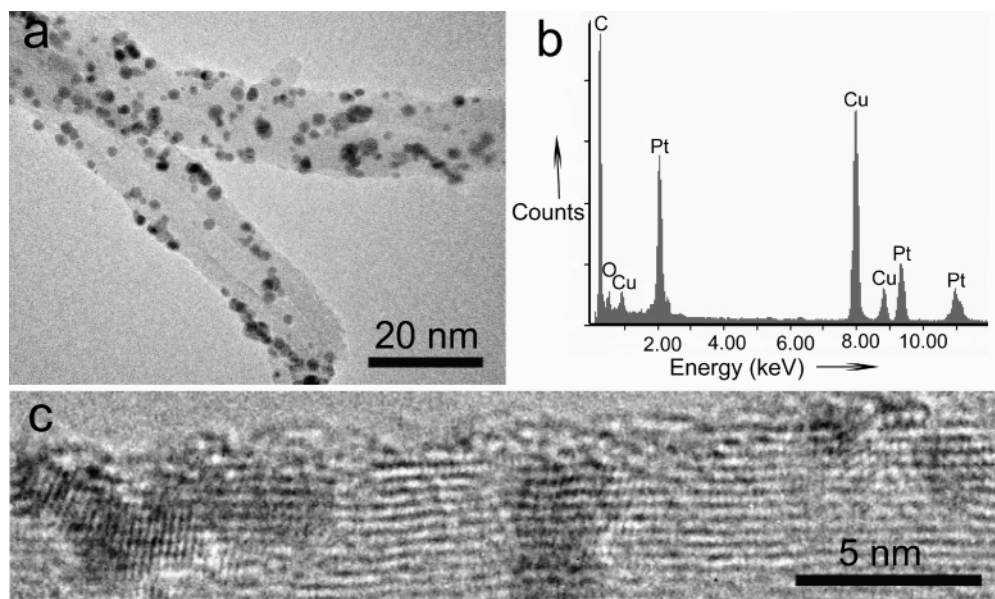


**Figure 3.** (a) TEM image of Pt/CNT composite (24.0 wt %) after thermal treatment at 400 °C for 1 h. (b) EDS from the Pt/CNT composite shown in panel a. (c) HRTEM image of the Pt/CNT composite shown in panel a.

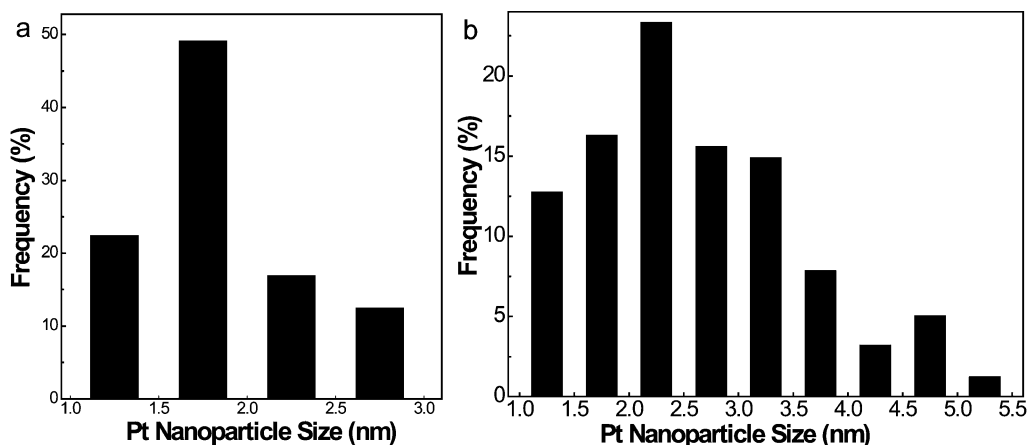


**Figure 4.** Size distribution of Pt nanoparticles on CNTs (a) before and (b) after thermal treatment.

the CNT surface. By adjusting the relative ratio of CNTs and Pt nanoparticles in toluene solution, different coverage of Pt nanoparticles on the CNT surface can be accomplished, which is crucial to their industrial applications as catalysts. The above results have clearly demonstrated the effectiveness of a simple route for the assembly of Pt nanoparticles on CNTs and that Pt nanoparticles are loaded on the outside walls of CNTs, not on the inside walls.

The Pt/CNT composite was investigated by annealing treatment because it is necessary to remove  $\text{PPh}_3$  molecules surrounding Pt nanoparticles before the Pt/CNT composite can be used as a catalyst. Figure 3a is the TEM image of Pt/CNT composite after thermal treatment at 400 °C for 1 h in ambient environment. The sample is the same as that shown in Figure 2b. The  $\text{PPh}_3$  protection layer on Pt nanoparticles should have been effectively removed because  $\text{PPh}_3$  decomposes at about 216 °C according to thermogravimetric analysis (not shown here). With the removal of  $\text{PPh}_3$ , Pt nanoparticles are fused and aggregate into larger particles. By comparing the size of Pt nanoparticles in Figures 2b and 3a, it is evident that Pt nanoparticles in Figure 3a are larger due to the aggregation of neighboring Pt nanoparticles after heat treatment. The average size of the Pt nanoparticles on CNTs before thermal treatment shown in Figure 2b is measured to be  $1.9 \pm 0.5$  nm, close to

that of Pt nanoparticles in toluene solution. Figure 4a is a statistical result from more than 200 Pt nanoparticles showing the distribution of the particle size. After thermal treatment, the mean particle size shown in Figure 3a is measured to be  $2.7 \pm 1.0$  nm and most Pt nanoparticles are smaller than 4 nm. Figure 4b is a statistical result from more than 200 Pt nanoparticles after heat treatment. From the results in Figure 4a,b, it is clear that the size distribution of Pt nanoparticles is quite narrow compared to previous reports.<sup>13,31</sup> After thermal treatment, Pt nanoparticles are still well dispersed, which is critical to their future application as catalysts. One of the advantages of thermal treatment is to increase the stability of the composite because the working temperature of DMFCs is much lower than the thermal treatment temperature. Figure 3b demonstrates the energy-dispersive X-ray spectroscopy (EDS) of the Pt/CNT composite shown in Figure 3a. The existence of elemental Pt can be clearly seen. Figure 3c is a high-resolution transmission electron micrograph (HRTEM) of the composite shown in Figure 3a, displaying a layer-by-layer morphology of the tube wall of the MWCNT and the crystalline facets of Pt nanoparticles, which demonstrate the highly crystalline character of metallic Pt particles.

The crystalline nature of the Pt nanoparticles was further confirmed by recording the X-ray power diffraction (XRD)

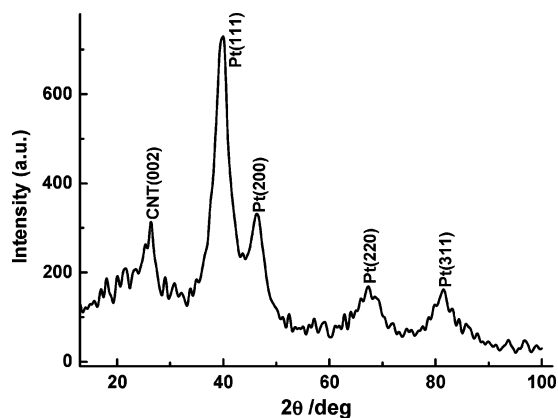


Figure 5. XRD pattern of Pt/CNT composite shown in Figure 4a.

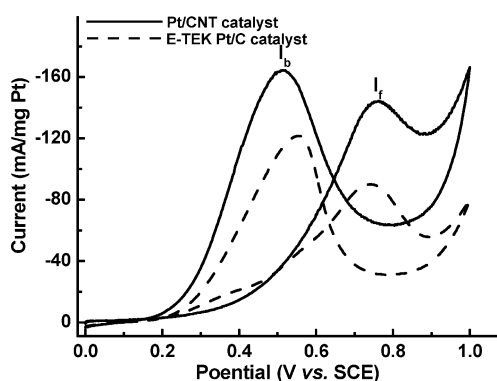
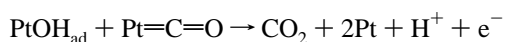


Figure 6. Cyclic voltammograms of methanol oxidation on Pt/CNT composite (solid line) and commercial E-TEK Pt/C catalyst (dash line) in 2 M CH<sub>3</sub>OH/1 M H<sub>2</sub>SO<sub>4</sub> electrolyte at 20 mV S<sup>-1</sup> at room temperature.

spectrum (Figure 5) of Pt/CNT composite after thermal treatment shown in Figure 3a. The peak at  $2\theta = 26.5^\circ$  corresponds to the (002) planes of graphitized CNTs. And the peaks at  $2\theta = 39.7^\circ$ ,  $46.2^\circ$ ,  $67.4^\circ$ , and  $81.2^\circ$  can be assigned to the (111), (200), (220), and (311) crystalline planes of fcc Pt, respectively, which indicates that the Pt nanoparticles are composed of pure crystalline Pt.

The electrochemical performance of the Pt/CNT composite (24 wt %, shown in Figure 3a) was tested for methanol oxidation, which is at the heart of DMFC application in the anodic half-cell reaction. For comparison, the commercial Pt catalyst (E-TEK, 20 wt %) was also employed. In Figure 6, the cyclic voltammograms for methanol oxidation at Pt/CNT composite prepared by our method (solid line) and the commercial catalyst (dash line) are compared. The voltammetric features are in good agreement with literature,<sup>6–8,18</sup> in which the typical methanol oxidation current peak on Pt catalyst is at about 0.74 V vs SCE in the forward scan. Figure 6 clearly shows that the oxidation current observed with Pt/CNT composite is considerably higher than that of the E-TEK catalyst. This significant improvement in the catalytic performance can be attributed to the high level of dispersion of Pt nanoparticles on CNTs. In the reverse scan, an oxidation peak is observed around 0.53 V, which is primarily associated with the removal of the residual carbon species formed in the forward scan.<sup>4,13,32,33</sup> The residual carbon species are oxidized according to the following reaction:



Therefore, the ratio of the forward oxidation current peak ( $I_f$ )

to the reverse current peak ( $I_b$ ),  $I_f/I_b$ , is an index of the catalyst tolerance to the poisoning species, Pt=C=O. A higher ratio indicates more effective removal of the poisoning species on the catalyst surface. The  $I_f/I_b$  ratio of Pt/CNT composite is 0.88, higher than that of the E-TEK catalyst (0.74), showing better catalyst tolerance of the Pt/CNT composite.

## Conclusions

In summary, a novel method has been successfully developed to load Pt nanoparticles on CNTs without pretreating the CNTs. It is unique in the system that the PPh<sub>3</sub> offers strong adhesion of Pt on CNT surface and sufficient protection for Pt nanoparticles from being aggregated. Pt/CNT composite with different Pt content was conveniently controlled by manipulating the relative concentration of CNTs vs Pt nanoparticles. Pt nanoparticles highly dispersed on CNTs kept their initial small sizes in solution. Even though thermal treatment led to some extent of aggregation of Pt nanoparticles, the sizes of most Pt nanoparticles are still smaller than 4 nm. The produced Pt/CNT composite shows higher electrocatalytic activities and catalyst tolerance that can be applied in DMFCs in comparison with the E-TEK catalyst. The present technique represents a highly feasible approach to produce Pt/CNT composite, which should have great potential in DMFC applications.

**Acknowledgment.** Financial support from National Natural Science Foundation of China (Nos. 20520140277, 20121301, and 20575070), National Key Project on Basic Research (Grant No. G2000077501), and Chinese Academy of Sciences is gratefully acknowledged.

## References and Notes

- Olah, G. A. *Angew. Chem., Int. Ed.* **2005**, *44*, 2.
- Winter, M.; Brodd, R. J. *Chem. Rev.* **2004**, *104*, 4245.
- Menicol, B. D.; Rand, D. A. J.; Williams, K. R. *J. Power Sources* **1999**, *83*, 15.
- Lamy, C.; Léger, J. M.; Srinivasan, S. *Mod. Aspects Electrochem.* **2001**, *34*, 73.
- Matsumoto, T.; Komatsu, T.; Arai, K.; Yamazaki, T.; Kijima, M.; Shimizu, H.; Takasawa, Y.; Nakamura, J. *Chem. Commun.* **2004**, 840.
- Yu, J. S.; Kanf, S.; Yoon, S. B.; Chai, G. *J. Am. Chem. Soc.* **2002**, *124*, 9382.
- Chen, W. X.; Lee, J. Y.; Liu, Z. L. *Chem. Commun.* **2002**, 2588.
- Liang, H. P.; Zhang, H. M.; Hu, J. S.; Guo, Y. G.; Wan, L. J.; Bai, C. L. *Angew. Chem., Int. Ed.* **2004**, *43*, 1540.
- Anderson, M. L.; Stroud, R. M.; Rolison, D. R. *Nano Lett.* **2002**, *2*, 235.
- Vinodgopal, K.; Haria, M.; Meisel, D.; Kamat, P. *Nano Lett.* **2004**, *4*, 415.
- Schmidt, T. J.; Paulus, U. A.; Gasteiger, H. A.; Behm, R. J. *J. Electroanal. Chem.* **2001**, *508*, 41.
- Bock, C.; Paquet, C.; Couillard, M.; Botton, G. A.; MacDougall, B. R. *J. Am. Chem. Soc.* **2004**, *126*, 8028.
- Liu, Z.; Ling, X. Y.; Su, X.; Lee, J. Y. *J. Phys. Chem. B* **2004**, *108*, 8234.
- Ebbesen, T. W.; Lezec, H. J.; Hiura, H.; Bennett, J. W.; Ghaemi, H. F.; Thio, T. *Nature* **1996**, *382*, 54.
- Baughman, R. H.; Zakhidov, A. A.; Heer, W. A. *Science* **2002**, *297*, 787.
- Lee, K. M.; Li, L. C.; Dai, L. M. *J. Am. Chem. Soc.* **2005**, *127*, 4122.
- Rajesh, B.; Thampi, K. R.; Bonard, J. M.; Xanthopoulos, N.; Mathieu, H. J.; Viswanathan, B. *J. Phys. Chem. B* **2003**, *107*, 2701.
- Guo, D. J.; Li, H. L. *J. Electroanal. Chem.* **2004**, *573*, 197.
- Tang, H.; Chen, J. H.; Huang, Z. P.; Wang, D. Z.; Rn, Z. F.; Nie, L. H.; Kuang, Y. F.; Yao, S. Z. *Carbon* **2004**, *42*, 191.
- Ang, L. M.; Andy Hor, T. S.; Xu, G. Q.; Tung, C. H.; Zhao, S.; Wang, J. L. S. *Chem. Mater.* **1999**, *11*, 2115.
- Yu, R. Q.; Chen, L. W.; Liu, Q. P.; Lin, J. Y.; Tan, K. L.; Ng, S. C.; Chan, H. S. O.; Xu, G. Q.; Andy Hor, T. S. *Chem. Mater.* **1998**, *10*, 718.

- (22) Rajalakshmi, N.; Ryu, H.; Shaijumon, M. M.; Ramaprabhu, S. *J. Power Sources* **2005**, 140, 250.
- (23) Li, W. Z.; Liang, C. H.; Zhou, W. J.; Qiu, J. S.; Zhou, Z. H.; Sun, G. Q.; Xin, Q. *J. Phys. Chem. B* **2003**, 107, 6292.
- (24) Kong, J.; Chapline, M.; Dai, H. *Adv. Mater.* **2001**, 13, 1384.
- (25) Bezryadin, A.; Lau, C. N.; Tinkham, M. *Nature* **2000**, 404, 971.
- (26) Choi, H. C.; Shim, M.; Bangsaruntip, S.; Dai, H. *J. Am. Chem. Soc.* **2002**, 124, 9058.
- (27) Girishkumar, G.; Vinodgopal, K.; Kamat, P. V. *J. Phys. Chem. B* **2004**, 108, 19960.
- (28) Nelson, T.; Vinodgopal, K.; Kumar, G. G.; Kamat, P. *Electrochem. Soc. Proc.* **2004**, 12, 152.
- (29) Quinn, B. M.; Dekker, C.; Lemay, S. G. *J. Am. Chem. Soc.* **2005**, 127, 6146.
- (30) Wang, Y.; Ren, J.; Deng, K.; Gui, L.; Tang, Y. *Chem. Mater.* **2000**, 12, 1622.
- (31) Xing, Y. *J. Phys. Chem. B* **2004**, 108, 19255.
- (32) Yajima, T.; Uchida, H.; Watanabe, M. *J. Phys. Chem. B* **2004**, 108, 2654.
- (33) Zhu, Y. M.; Uchida, H.; Yajima, T.; Watanabe, M. *Langmuir* **2001**, 17, 146.